Graphite Sheet Coating for Improved Thermal Oxidative Stability of Carbon Fiber Reinforced/ PMR-15 Composites

Sandi Campbell[1], Demetrios Papadopoulos[2], Paula Heimann[3], Linda Inghram[3] and Linda McCorkle[3]

[1]NASA Glenn Research Center, Cleveland, OH. 44135

[2]University of Akron, Department of Polymer Science, Akron, OH

[3]Ohio Aerospace Institute, Cleveland, OH
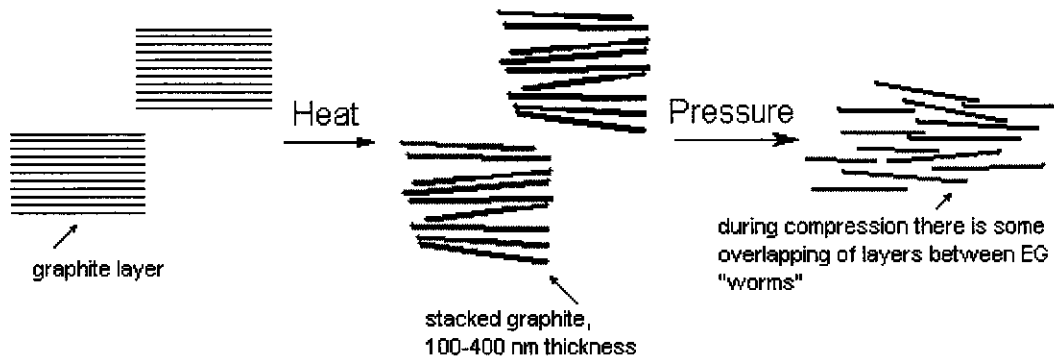
Abstract

Expanded graphite was compressed into graphite sheets and used as a coating for carbon fiber reinforced PMR-15 composites. BET analysis of the graphite indicated an increase in graphite pore size on compression, however the material was proven to be an effective barrier to oxygen when prepregged with PMR-15 resin. Oxygen permeability of the PMR-15/graphite was an order of magnitude lower than the compressed graphite sheet. By providing a barrier to oxygen permeation, the rate of oxidative degradation of PMR-15 was decreased. As a result, the composite thermo-oxidative stability increased by up to 25%. The addition of a graphite sheet as a top ply on the composites yielded little change in the material's flexural strength or interlaminar shear strength.

Introduction

There has been a constant drive to increase the use temperature and extend the high temperature lifetime of polymers for aerospace components.[1-4] As a result, considerable effort has been made to elucidate the degradation mechanisms of the state of the art high temperature polymers, such as, PMR-15.[5-9] It has been reported that PMR-15 follows an oxidative degradation process. On high temperature aging, a layer of oxidized polymer forms on the surface of the resin. Continued aging leads to cracking within the oxidation layer, allowing diffusion of oxygen into the bulk polymer and furthering oxidative degradation. Therefore, slowing the diffusion of oxygen into the bulk polymer can improve the thermo-oxidative stability of the material.[10-12]

Layered silicates have been added to numerous polymer systems to slow the gas permeability.[13-17] Recently, expanded graphite has been attracting attention as an analogous material.[18-19] Expanded graphite (EG) is prepared by rapid heating of a graphite intercalation compound, (graphite flakes containing H_2SO_4/HNO_3 between the planes). EG is a light, porous, vermiculite-like material, composed of stacked graphite planes. The individual planes of EG have a high aspect ratio and dispersion of the sheets in a polymer matrix may result in a reduction in gas diffusion similar to that observed with layered silicates.[20]

Rather than dispersing EG into a matrix, it can also be compressed into flexible graphite sheets. On compression, there is overlap and mechanical interlocking of the sheets, which may further impede gas diffusion. The schematic below illustrates the expansion and compression of a graphite intercalation compound.[21]

graphite layer

Heat

stacked graphite,
100-400 nm thickness

Pressure

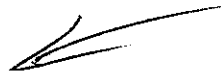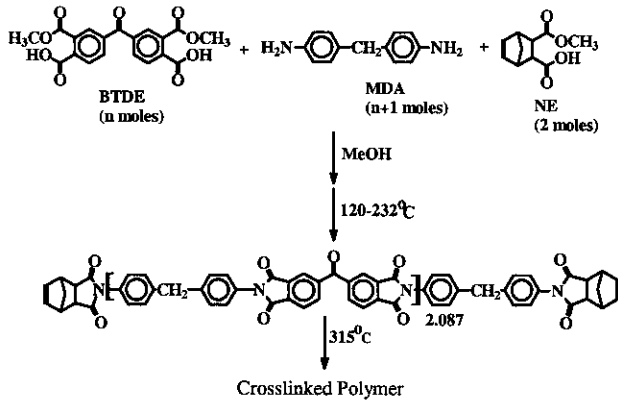during compression there is some
overlapping of layers between EG
"worms"

Fig 1 and caption

In this paper, we describe the oxygen permeability of a compressed graphite sheet and a PMR-15/graphite sheet, and their influence on the thermal and mechanical properties of PMR-15 matrix composites.

Experimental

Materials: Methylene dianiline (MDA) was purchased from Aldrich Chemical Company. Nadic anhydride (NA) was acquired from TCI America. 3,3',4,4'-benzophenonetetracarboxylic acid dianhydride (BTDA) was purchased from Chriskev. Expandable graphite was received from Graftec. All materials were used as received.

Synthesis: PMR-15 synthesis is illustrated in Figure 1. The acid-ester of BTDA (BTDE) was prepared by refluxing BTDA in methanol. Reflux continued for two hours following dissolution of the dianhydride.[22] The amount of methanol was calculated to yield a solution containing 50 wt% solids.

BTDE (n moles) + **MDA** (n+1 moles) + **NE** (2 moles)

MeOH

120-232°C

2.087

315°C

Crosslinked Polymer

Neat resin synthesis: The three monomers (BTDE, MDA, and NE) were dissolved in methanol (50 wt%) followed by solvent evaporation, on a hot plate, at 60° to 70°C. B-staging the mixture at 204° to 232°C in an air circulating oven produces a low molecular weight imide oligomer. This oligomer was then cured in a mold for two hours at 315°C under 2355 psi to produce a crosslinked polymer. The polymer was post cured in an air circulating oven for 16 hours at 315°C to further crosslinking. The average number of imide rings was kept constant by using a stoichiometry of 2NE/ (n+1)MDA/ nBTDE (n=2.087) corresponding to an average molecular weight of 1500.

Composite Preparation: PMR-15 monomers (BTDE, MDA, and NE) were dissolved in methanol with a solids content of approximately 50 wt%. Composite prepreg was prepared by brush application of the PMR-15 monomer solution onto T650-35 carbon fabric, to give a final fiber content of 60 wt%. The prepreg sheets were cut into eight, 10.2 cm by 10.2 cm, plies and placed in a metal mold. The prepreg was B-staged at 204° to 232°C in an air circulating oven, then cured in a mold for two hours at 315°C under 500 psi. The composites were post cured in an air circulating oven at 315°C for 16 hours.

Expanded Graphite: Expandable graphite was placed in an oven which had been preheated to 700°C. The graphite expanded in seconds, but was left in the oven for two minutes to ensure removal of the intercalated acid.

Preparation of Graphite Sheets: Compressed graphite sheets were prepared by placing 1g of expanded graphite between Kapton sheets in a 10.16 cm x 10.16 cm mold. The mold was placed in a hydraulic press at room temperature, and 1000 psi was applied for 15 minutes. The compressed sheet was easily peeled from the Kapton. For this paper, compressed sheets composed of only expanded graphite will be referred to as neat graphite sheets, (NGS). A second set of compressed sheets were prepared by stirring 1g of expanded graphite with 1g of PMR-15 monomer solution. The monomer solution contained a minimal amount of methanol. The expanded graphite/monomer solution was placed between Kapton sheets in a 10.16 cm x 10.16 cm mold, and the compressed sheet was prepared as described above. These compressed graphite sheets will be referred to as monomer graphite sheets (MGS).

Graphite coated composites were prepared by applying either NGS or MGS as a top ply to the PMR-15 matrix composites. Three separate batches of uncoated and coated composites were prepared and characterized. The coated composites were processed following the PMR-15 composite processing procedure described above.

Characterization

BET analysis was performed using a Micromeritics ASAP2010 Surface Area / Pore Analyzer. The analysis gas was nitrogen and the samples were out gassed at 200°C overnight.

Ultrasonic scanning (C-scan) was used to characterize composite quality. Void content was measured by acid digestion, in accordance with ASTM Standard D792.

Isothermal aging of PMR-15 composites was performed to determine the thermo-oxidative stability (TOS). Post-cured samples were cut into 2.54 cm by 1.27 cm coupons and placed in an air circulating oven at 288°C for 1000 hours. The weight loss was measured at regular intervals by removing the coupons from the oven, allowing them to cool to room temperature, and weighing the sample.

Oxygen Permeability tests were performed at the Tulane Institute for Macromolecular Engineering and Science (TIMES). The tests were carried out in a pressure cell designed according to the ASTM Designation: D 1434-82. The pressure cell was modified by replacing the manometric cell with a pressure transducer. The membrane being tested was sealed within the pressure cell, and divided the cell into two chambers. One chamber was kept at a constant high oxygen pressure; the other side was initially at atmospheric pressure. Since the volume of the chamber at the downstream (low pressure side) was almost constant during the test, the amount of oxygen transport through the membrane could be calculated from the pressure change at the (low pressure) downstream side.

Flexural strength, flexural modulus, and interlaminar shear strength of carbon fabric reinforced composites were measured using an Instron model 4505 and Series IX acquisition software. A 3- point flexure test, ASTM D790, was used to evaluate flexural strength and modulus. Short beam shear tests followed ASTM D2344, for measurements of interlaminar shear strength.

Results and Discussion

The changes in graphite morphology on expansion and compression were
characterized by SEM, and are shown in Figure 2. The graphite intercalation compound
was characterized as randomly arranged, overlapping graphite flakes. This was in
contrast to the expanded graphite "worms", in which separate groups of graphite planes
were observed.[23]
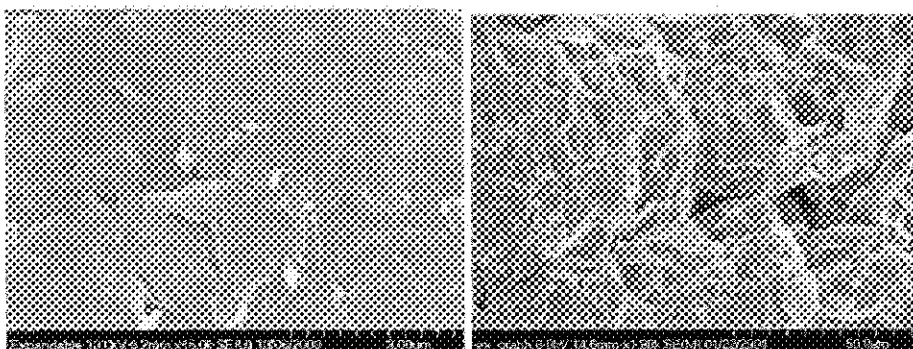
The graphite flakes were also visible in the compressed graphite sheet. However, as
opposed to the expandable graphite, the layers of the compressed sheet are densely
packed.
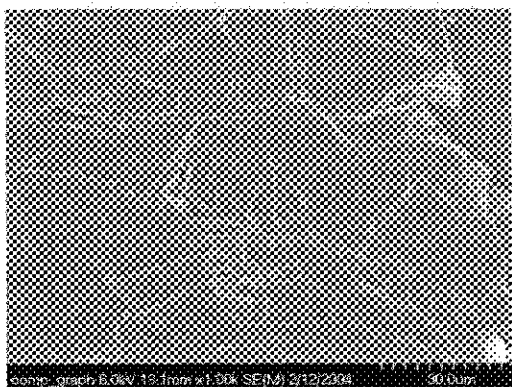
The surface area and pore diameter of the graphite intercalation compound, the
expanded graphite, and the compressed graphite sheet were determined by BET analysis.
The results are listed in Table 1.

Sample	Surface Area (sq. m/g)	Pore Volume (cc/g)	Avg. Pore Diameter (A)
Graphite intercalation compound	10.55	0.01	42.4
Expanded (EG)	141.67	0.14	39.9
Compressed (NGS)	11.09	0.05	147.7

A 10 fold increase in the graphite surface area was observed on expansion of the graphite intercalation compound. This was attributed to the high degree of separation between the graphite planes in the expanded material. The pore diameter does not change on expansion. Compression of EG into sheets decreases the surface area, and greatly increases the pore diameter.

The worm-like particles of EG contain two kinds of porosity. The interparticle porosity corresponds to the fraction of pore space between the graphite worms, while the intraparticle porosity is located within each worm.[21] At the beginning of compaction, the worms rearrange spatially, but only a small fraction of the interparticle porosity is removed. Because of the mechanical interlocking, the worms do not move enough to remove all interparticle porosity.[21] As a result, the compressed graphite sheet has a large pore diameter.

Permeability

BET analysis confirmed that the compressed graphite is porous, and therefore should be too permeable for the purpose of an oxygen barrier coating. However, the addition of PMR-15 to EG before compression should lower the film's permeability by filling the pores of the graphite sheet. Oxygen permeability measurements were used to evaluate the efficiency of the films at slowing the oxygen diffusion. Figure 3 shows the permeability data for NGS, and MGS.
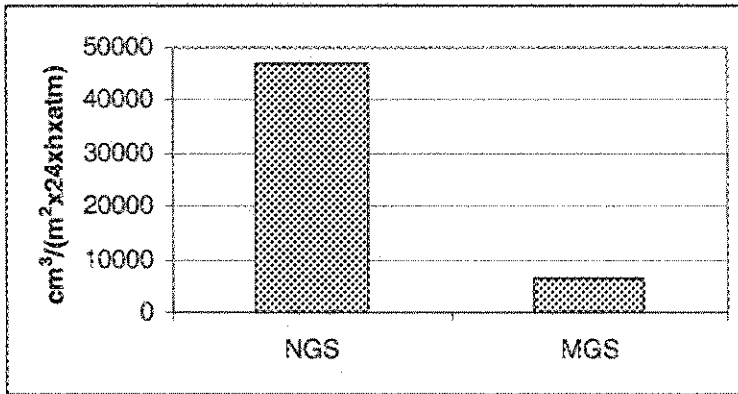
The data shows that addition of PMR-15 to the compressed graphite sheet lowers the permeability of NGS by an order of magnitude.

The decrease in gas permeability that is observed on dispersion of a platelet-like filler in a matrix has been widely described by the tortuous path model.[24-25] Briefly, the model states that by dispersing high aspect ratio materials throughout a matrix, the path length of a permeant is increased, thereby slowing diffusion.

This model has also been applied to gas permeability through a graphite sheet.[26] It has been observed that increasing the bulk density of the sheet increases tortuosity. The density of the sheets prepared in this study was constant for all samples, and therefore the tortuosity and resultant gas permeability will depend on the overlapping of graphite planes during compaction and the resultant pore size.

Thermal Stability

PMR-15 neat resin disks were coated on one side with graphite, and the thermo-oxidative stability of the resin was evaluated. The aging data revealed a 21% decrease in weight loss for resin coated with MGS. Coating with NGS resulted in a 15% decrease,

which is significant, but lower than MGS. Figure 5 plots the weight loss of each sample
after 1000 hours of aging at 288°C.
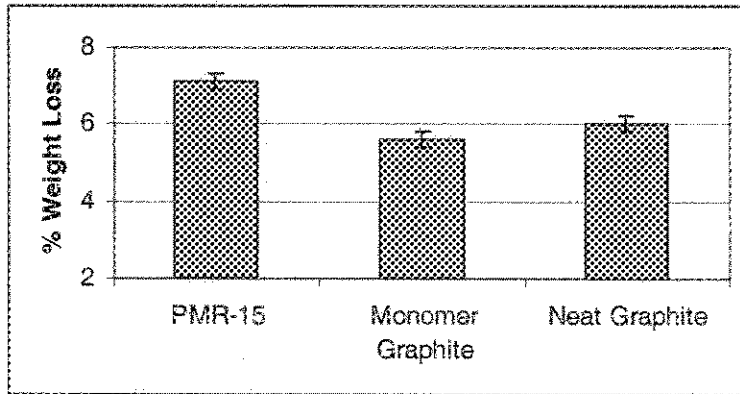
The oxidation of the aged PMR-15 resin is clearly visible by optical microscopy as a
white layer forming on the surface of the sample. Figure 6 shows the oxidation of
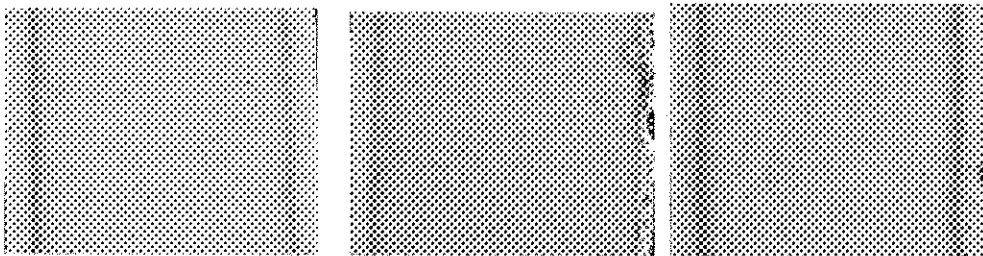uncoated PMR-15, MGS coated, and NGS coated.

Figure 6b and 6c shows the MGS and the NGS, respectively, on the right hand side of the
resin. Coating with MGS provided the best protection from oxidation. The microscopy
image shows no oxidation of the sample under the coating, except for a small region
where the coating was damaged. This is not the case for the NGS coated resin. In this
sample, there is a layer of oxidized resin below the coating. These results are expected
based on the oxygen permeability data of the NGS and MGS films. NGS is very
permeable to oxygen while MGS is not. The absence of an oxidation layer below the
MGS demonstrates the low permeability of this sheet. By slowing the diffusion of

oxygen, the coating decreases the oxidation of the resin, thereby increasing the thermo-
oxidative stability.

Similar results were found when coating carbon fiber reinforced composites.
Applying MGS as a top ply of the carbon fiber reinforced composites decreases the
weight loss on aging by approximately 25%. The NGS lowers the weight loss by only
7%.
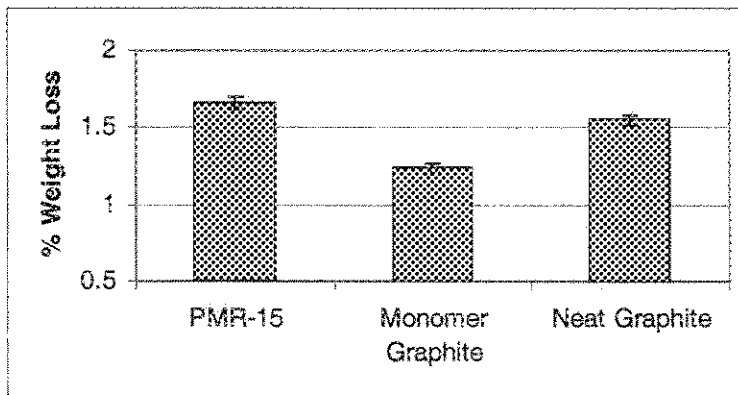
The oxidation of PMR-15 is clearly visible by optical microscopy, as shown in Figure 8.
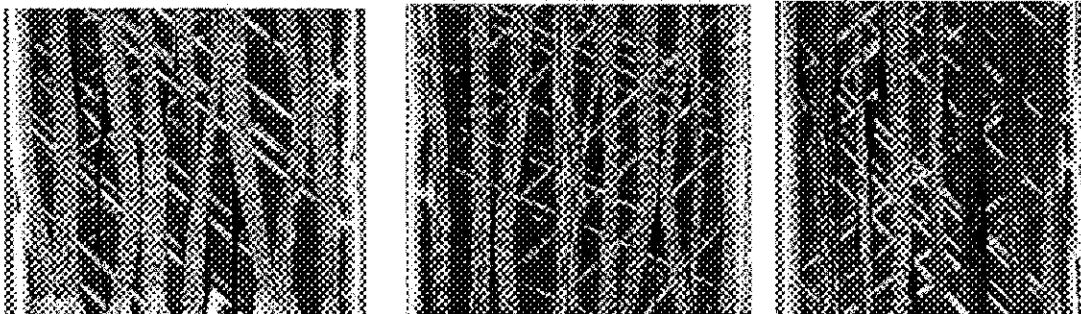

Figure 8a shows the formation and cracking of an oxidation layer on a thermally aged
PMR-15 composite. Figure 8b and 8c shows the MGS and the NGS, respectively, on the
right hand side of the composites. The composite coated with MGS shows little
oxidation and no cracking under the graphite, while cracking was observed on the
opposite edge of the sample. There was significant cracking and oxidation under the

NGS coating resulting in little improvement in the materials thermal stability compared to the base composite.

Addition of MGS or NGS as both top and bottom plies of the PMR-15 composites results in a 20% decrease in weight loss, in both cases. It is unclear why both graphite sheets give similar weight loss in this case.

Composite Mechanical Properties

The data from specified mechanical tests are listed in Table 2.

Sample	Flexural Strength	Flexural Modulus	Interlaminar Shear Strength
PMR-15	143 $^+$/. 8	9.08 $^+$/. 0.2	10048 $^+$/. 404
Monomer-Graphite Coated	141$^+$/. 9	7.95 $^+$/. 0.16	9639 $^+$/. 401
Graphite Coated	127 $^+$/. 7	7.7 $^+$/. 0.22	9541 $^+$/. 594

There was not a significant change in the interlaminar shear strength of the composites. The shear strength should remain unchanged when the coating is added, because failure by this mechanism originates between composite plies. The microscopy images shown in Figure 9 reveal no damage to the coating after testing, indicating the failure mechanism of the composite was not affected by the presence of the coating.
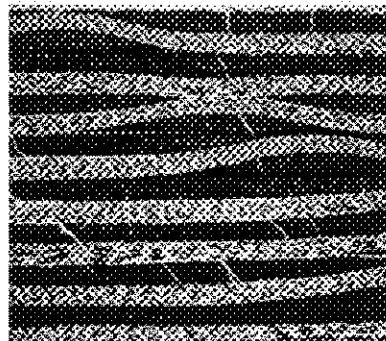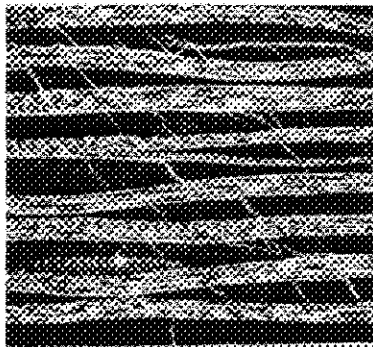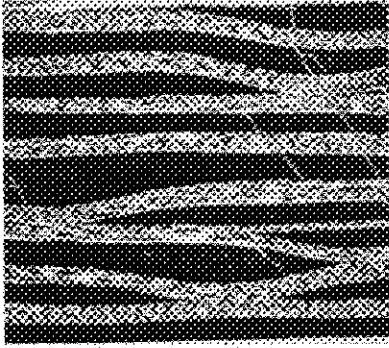
The results of the flexural testing show a drop-off in the modulus of both coated samples, and a decrease in the flexural strength of NGS. The microscopy images of the fractured composites are shown in Figure 10.
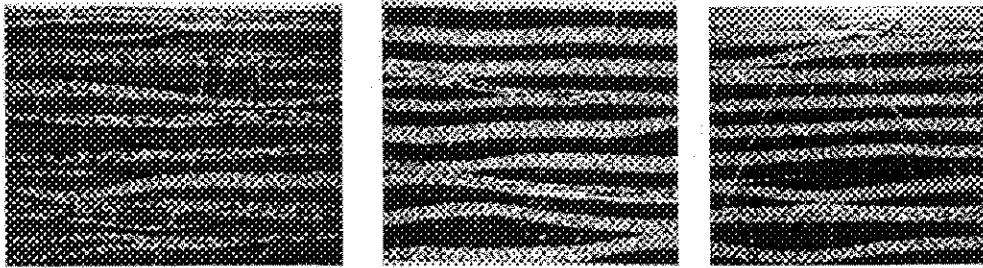
Figures 10b and 10c show the MGS and the NGS, respectively, on the top of the composites. The images show considerable damage to the NGS coating during fracture, while the MGS coating remains intact. Studies on the fracture mechanism of flexible graphite sheets have shown that fracture is initiated by cleavage between the graphite planes near the surface of the sheet. The sheet is broken when the planes slip and separate.[27] Figure 10c shows significant damage to the NGS coating after fracture. This damage was not seen in the MGS coating. The addition of the PMR-15 monomers as a binder in the MGS prevents the slipping of the graphite planes, resulting in a flexural strength identical to that of PMR-15.

It should be noted that the graphite sheets contribute to the dimensions of the sample. The ~0.05cm increase in specimen thickness, compared to the uncoated material, may contribute to a reduction in calculated strength.

Conclusions

Compressed graphite sheets were added as a top ply to a PMR-15 matrix composite. The graphite sheets were prepared from either expanded graphite, or expanded graphite mixed with a PMR-15 monomer solution. The oxygen permeability of the compressed graphite (NGS) was high, due to the high porosity of this material. The permeability was further decreased by incorporating PMR-15 into the graphite sheet (MGS). By providing an efficient barrier to oxygen, the high temperature thermo-oxidative stability of the composites was increased. The coatings, in particular MGS, had little to no effect on the mechanical properties of the composite.

Acknowledgements

References

1. J.G. Smith Jr., J.W. Connell, P.M. Hergenrother, L.A. Ford, and J.M. Criss, *Macromol. Symp.* **2003**, *199*, 401-418.

2. J.Y. Hao, A.J. Hu, S.Q. Gao, X.Ch. Wang, and S.Y. Yang, *High Perform. Polym.* **2001**, *13*, 211-224.

3. R. Magaraphan, W. Lilayuthalert, A. Sirivat, and J. Schwank, *Composites Sci. and Tech.* **2001**, *61*, 1253-1264.

4. D. Wilson, *High Perform. Polym.* **1991**, Vol 3, No 2, 73- 87.

5. M.A.B. Meador, J.C. Johnston, A. Frimer, and P. Gilinsky-Sharon, *Macromolecules* **1999**, *32*, 5532-5538

6. S. Tamai, W. Yamashita, and A. Yamaguchi, *J. Polym. Sci: Part A: Polym. Chem.*, **1998**, *36*, 1717-1723.

7. M.J. Turk, A. Ansari, W.B. Alston, G. Gahn, A. Frimer, and D. Scheiman, *J. Polym. Sci: Part A: Polym. Chem.*, **1999**, *37*, 3943-3956.

8. W. Xie, R. Heltsley, X. Cai, F. Deng, J. Liu, C. Lee, and W.-P. Pan, *J. of Appl. Polym. Sci.*, **2002**, *83*, 1219-1227.

9. J.P. Habas, J. Peyrelasse, and M.F. Grenier-Loustalot, *High Perform. Polym.*, **1996**, *8*, 579-598.

10. L.L. Johnson, R.K. Eby, and M.A.B. Meador, *Polymer*, **2003**, *44*, 187-197.

11. M.A.B. Meador, C. Lowell, P. Cavano, and P. Herrera-Fierro, *High Perform. Polym.*, **1996**, *8*, 363-379.

12. K.J. Bowles, D. Papadopoulos, D. Scheiman, L. Inghram, L. McCorkle, O. Klans, *NASA Technical Memorandum* 211878, May 2003.

13. C. Nah, H.J. Ryu, W.D. Kim, and S.S. Choi, Polym. Adv. Technol. **2002**, 13, 649-652.

14. P. Messersmith and E.P. Giannelis, *J. Polym. Sci: Part A: Polym. Chem.*, **1995**, *33*, 1047-1057.

15. J.-H. Chang and Y. Uk An, *J. Polym. Sci: Part B: Polym. Phys.*, **2002**, *40*, 670-677.

16. G. Gorrasi, M. Tortora, V. Vittoria, G. Galli, and E. Chiellini, *J. Polym. Sci: Part B: Polym. Phys.*, **2002**, *40*, 1118-1124.

17. G. Gorrasi, M. Tortora, V. Vittoria, G. Galli, E. Pollet, B. Lepoittevin, M. Alexandre, and P. Dubois, *Polymer*, **2003**, *44*, 2271-2279.

18. M. Xiao, L. Sun, J. Liu, Y. Li, and K. Gong, *Polymer* **2002**, *43*, 2245-2248.

19. Y.-X. Pan, Z.-Z. Yu, Y.-C. Ou, and G.-H. Hu *J. Polym. Sci: Part B: Polym. Phys.*, **2000**, *38*, 1626-1633.

20. G. Chen, D. Wu, W Wen, and C. Wu *Carbon* **2003**, *41*, 619-621.

21. A. Celzard, S. Schneider, J.F. Mareche *Carbon*, **2002**, *40*, 2185-2191.

22. T. Serafini, P. Delvigs and G. Lightsey, *J. Appl. Poly. Sci.*, 16, 905 (1972).

23. G. Chen, C. Wu, W. Weng, D. Wu, and W. Yan, *Polymer*, **2003**, *44*, 1781-1784.

24. R.K. Bharadwaj, Macromolecules, 2001, 34, 9189-9192

25. A. Gusev, and H.R. Lusti, Adv. Mater. 2001, 13, No. 21, pg 1641-1643.

26. S. Biloe, and S. Mauran, Carbon 41 (2003) 525-537

27. Gu J., et al, Carbon 40 (2002) 2169-2176

Figures and Tables

Figure 1: PMR-15 synthesis

Figure 2: SEM images of graphite intercalation compound, expanded graphite, compression molded graphite.

Figure 3. Oxygen permeability data for PMR-15, NGS and MGS

Figure 4- schematic illustrating the compaction. (removed)

Figure 5- Weight Loss on aging (neat resin)

Figure 6- optical microscopy of neat resin

Figure 7- Weight Loss on aging

Figure 8- Optical Microscopy of the aged samples.

Figure 9 – SEM images of the shear samples.

Figure 10- SEM images of the flex samples.

Table 1: BET data

Table 2- Flex and shear data